Nanoscale Res Lett (2010) 5:853–858
DOI 10.1007/s11671-010-9574-5

NANO EXPRESS

Tunable Magnetic Properties of Heterogeneous Nanobrush: From Nanowire to Nanofilm

Y. Ren · Y. Y. Dai · B. Zhang · Q. F. Liu · D. S. Xue · J. B. Wang

Received: 16 January 2010 / Accepted: 1 March 2010 / Published online: 14 March 2010

Abstract With a bottom-up assemble technology, heterogeneous magnetic nanobrushes, consisting of Co nanowire arrays and ferromagnetic $Fe_{70}Co_{30}$ nanofilm, have been fabricated using an anodic aluminum oxide template method combining with sputtering technology. Magnetic measurement suggests that the magnetic anisotropy of nanobrush depends on the thickness of $Fe_{70}Co_{30}$ layer, and its total anisotropy originates from the competition between the shape anisotropy of nanowire arrays and nanofilm. Micromagnetic simulation result indicates that the switching field of nanobrush is 1900 Oe, while that of nanowire array is 2700 Oe. These suggest that the nanobrush film can promote the magnetization reversal processes of nanowire arrays in nanobrush.

Keywords Nanobrush · Anisotropy · Micromagnetic simulation

Introduction

With the development of nanotechnology, magnetic materials with different shapes have been studied widely for their importance to fundamental research and potential technological applications recently [1–4]. Nanomaterials including magnetic materials have been defined as zero-dimensional nanoparticle, one-dimensional nanowire, and two-dimensional nanofilm. Their special low-dimensional structures cause their unique physical and chemical properties especially magnetic properties compared with their bulk materials [5–8]. Among these nanomaterials, magnetic nanowire arrays have been attracted much attention on their significance about the magnetization reversal mechanism, high density magnetic recording media, or sensor [9–13]. The properties and applications of magnetic nanowire arrays are mainly determined by their magnetic anisotropy. Generally, magnetic nanowire arrays have uniaxial anisotropy along the long axis of wire for their shape anisotropy, so it is hard to change their total anisotropy for a certain magnetic nanowire arrays with fixed length and diameter. Fortunately, hexagonally close-packed (HCP) Co nanowire array has strong magnetocrystalline anisotropic constant that is comparable with its shape anisotropic constant; this gives us a chance to adjust the total anisotropy of magnetic nanowire array via changing the preferred growth orientation of HCP Co nanowire array. Up to now, many groups attempt to adjust the magnetic anisotropy of Co nanowire arrays via adjusting their microstructure or multilayer nanowire arrays [10, 14, 15]. In these cases, the total anisotropy of nanowire arrays increases if the direction of magnetocrystalline anisotropy is parallel to that of the shape anisotropy, while decreases if they are perpendicular to each other [15]. However, it is not very easy to obtain HCP Co nanowire arrays with expected microstructure or crystalline texture, and it is still a challenge to change the easy magnetization direction of the arrays of other materials with lower magnetocrystalline anisotropic constant, for example, Ni, Fe, or other magnetic alloys [16–18]. Nanobrush can

Y. Ren · Y. Y. Dai · B. Zhang · Q. F. Liu · D. S. Xue · J. B. Wang (✉)
Key Laboratory for Magnetism and Magnetic Materials of Ministry of Education, Lanzhou University, 730000 Lanzhou, People's Republic of China
e-mail: wangjb@lzu.edu.cn

J. B. Wang
Key Laboratory of Low Dimensional Materials and Application Technology, Xiangtan University, 411105 Xiangtan, People's Republic of China

be regarded as a combination of nanofilm and nanowire arrays, and it is studied as one of the nanodevices with high efficiency function made of nanowires of other nanostructures [19–22]. In this paper, magnetic nanobrushes, made of Co nanowire arrays and $Fe_{70}Co_{30}$ nanofilm, have been fabricated firstly to study the tunable magnetic anisotropy. Magnetic measurement indicates that the magnetic anisotropy of nanobrush can be adjusted by the thickness of $Fe_{70}Co_{30}$ layer. Micromagnetic simulation was also used to study the magnetization reversal process of the nanobrush compared with nanowire array.

Experimental Section

Magnetic nanobrushes, which consist of Co nanowire arrays and $Fe_{70}Co_{30}$ nanofilm, have been fabricated via AC voltage electrodeposition combining with sputtering technology. AAO template was prepared by anodic oxidation of 99.999% pure Al sheet undergone a two-step anodizing process in oxalic acid solution [23]. The process of fabricating AAO template is similar to our previous study [10]. Especially, the Al foils were anodized in 25.6 g l^{-1} $H_2C_2O_4$ solution under a constant DC voltage of 40 V for 3 h in the second anodizing step. Second, the cobalt nanowire arrays were electrodeposited into pores of the AAO template. Using a standard double electrode bath, the Al with AAO template was used as one electrode and the graphite as another. The electrolyte consisted of 0.3 M $CoSO_4$ and 45 g l^{-1} boric acid with $p\mathrm{H} = 3$ [14]. In addition, ac electrodeposition was conducted at 200 Hz, 12 V for 5 min. Third, the surface of the template was smoothed by dilute nitric acid solution. And then, a layer of $Fe_{70}Co_{30}$ was sputtered on one side of the Co nanowire array through a sputtering technique. After that, the Al substrate and the other cobalt nanowire arrays were removed by $HgCl_2$ solution. At last, nanobrush containing Co nanowire arrays and a $Fe_{70}Co_{30}$ layer was obtained nominally. The process of preparing the nanobrush was described in Fig. 1.

Scanning electron microscopy (SEM, Hitachi-S4800, Japan) was used to investigate the morphology of the AAO template and nanobrush. The magnetic properties were measured using a vibrating sample magnetometer (VSM, Lakeshore 7304, USA) at room temperature. Micromagnetic simulations are performed with the three-dimensional (3D) object oriented micromagnetic framework (OOMMF) method [10]. We simulated nanobrush consisting of nanowire arrays with amount of sixteen, the diameter of 20 nm and length of 400 nm and FCC Co nanofilm with the thickness of 12 nm. The unit cell size is 2.5 × 2.5 × 2.5 nm^3, which is approximately the same as the exchange length, $l_{ex} \propto \sqrt{2A/\mu_0 M_s^2}$.

Results and Discussion

The morphologies of the AAO templates and nanobrush are shown in Fig. 2. Figure 2a, b show the typical top view and side view of AAO template, respectively. The straight nanoholes with average diameter around 50 nm demonstrate a symmetrical distance for each other, which is propitious to gain regular nanowire arrays. It can be found in Fig. 2c, d that nanowires are filling into the porous of AAO template and parts of nanowires appear after etching AAO template by using NaOH solution. After sputtering $Fe_{70}Co_{30}$ layer on one side of the nanowire arrays membrane, magnetic nanobrush with AAO template can be obtained nominally as in Fig. 1. It is worthy to note that nanowire arrays are about 3 μm long with diameter of 50 nm, and the thickness of nanofilm is lower than 60 nm; thus, Co nanowire array is still the main body of nanobrush.

Figure 3a shows the normalized loops of Co nanowires, nanobrushes with different thickness of $Fe_{70}Co_{30}$ layer, and $Fe_{70}Co_{30}$ nanofilm with the applied field perpendicular to the plane of membrane. The coercivity and Sq (M_r/M_s) as a function of the thickness of nanofilm have been described in Fig. 3b. It is found that the coercivity and Sq are the largest for cobalt nanowire arrays, decrease regularly with the increase of thickness of $Fe_{70}Co_{30}$ layer, and smallest as the thickness reaches 60 nm. Subsequently, the coercivity and Sq of $Fe_{70}Co_{30}$ nanofilm with the thickness of 60 nm were drawn too, it has lower coercivity and Sq compared with nanobrushes. This indicates that the static magnetic properties of nanobrush can be controlled by changing the thickness of ferromagnetic layer like $Fe_{70}Co_{30}$ layer. On the other hand, Fig. 4a shows the normalized loops of samples mentioned above under the applied field parallel to the plane of membrane. The coercivity and Sq of nanowire as a function of the thickness of $Fe_{70}Co_{30}$ layer were drawn in Fig. 4b. It demonstrates that the coercivity of nanobrushes decreases regularly as increasing the thickness of $Fe_{70}Co_{30}$ layer, which is similar to the results as the applied field perpendicular to the surface of membrane. Furthermore, the Sq increases regularly as the thickness of $Fe_{70}Co_{30}$ layer increasing. The coercivity and Sq of nanobrush are nearly equal to those of $Fe_{70}Co_{30}$ film with the thickness of 60 nm. It indicates that the magnetic properties of nanobrush can be seen as the transition from nanowire to nanofilm. As well known, the magnetic moment distribution of ideal magnetic nanowire is almost along the long axis of nanowire for its strong shape anisotropy; thus, its easy magnetization direction will be parallel to the long axis of nanowire and hard magnetization direction perpendicular to its long axis. For nanofilm, its magnetic moments lie in the surface of membrane, which results in an in-plane easy magnetization direction

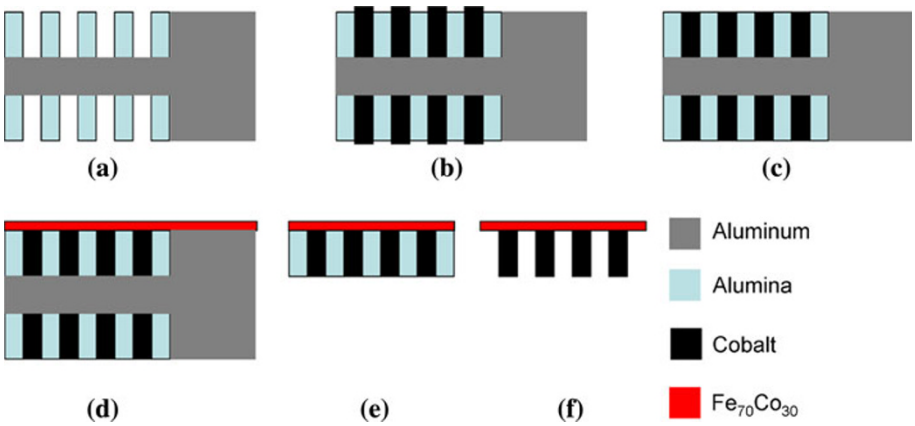

Fig. 1 Preparation scheme of magnetic nanobrush. **a** The AAO template covered with Al was fabricated by anodization of Al film in an acidic solution. **b** Cobalt nanowires were electrodeposited into the nanoporous. **c** The surface of film was smoothed by dilute nitric acid solution. **d** The surface of film was covered with a $Fe_{70}Co_{30}$ layer by the sputtering technique. **e** Al substrate and another cobalt nanowire arrays were removed by $HgCl_2$ solution. **f** After eroding the AAO template using NaOH solution, a nanobrush was obtained

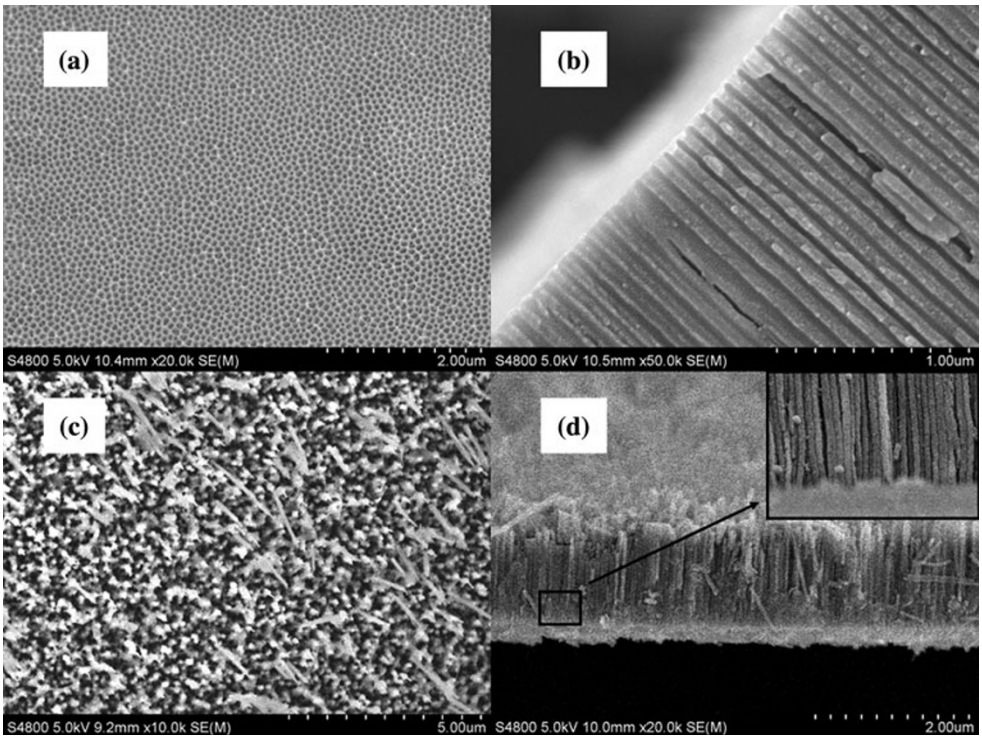

Fig. 2 SEM images: **a** top view, **b** side view of AAO template, **c** top view, and **d** side view of the nanobrush with wire diameter of 50 nm

and an out-of-plane hard magnetization direction. To investigate the relationship between magnetic anisotropy and the thickness of $Fe_{70}Co_{30}$ layer of nanobrush, the effective anisotropy fields of nanobrush were calculated [24], and listed in Table 1.

Table 1 indicates that nanowire array and nanobrush with 20 nm thickness of $Fe_{70}Co_{30}$ layer show easy-axis type of anisotropy, and their easy magnetization direction is along the long axis of nanowire, whereas nanobrush with $Fe_{70}Co_{30}$ layer higher thickness and nanofilm are easy-plane type of anisotropy will be magnetized easily in the film plane. The transition from easy-axis type to easy-plane type can be obtained as the thickness of $Fe_{70}Co_{30}$ layer increases. We also find that the effective easy-axis anisotropy field decreases from nanowire arrays to Sample A, while the effective easy-plane anisotropy field increases as the thickness of $Fe_{70}Co_{30}$ layer increases. Therefore, it is an effective method to control the magnetic anisotropy of

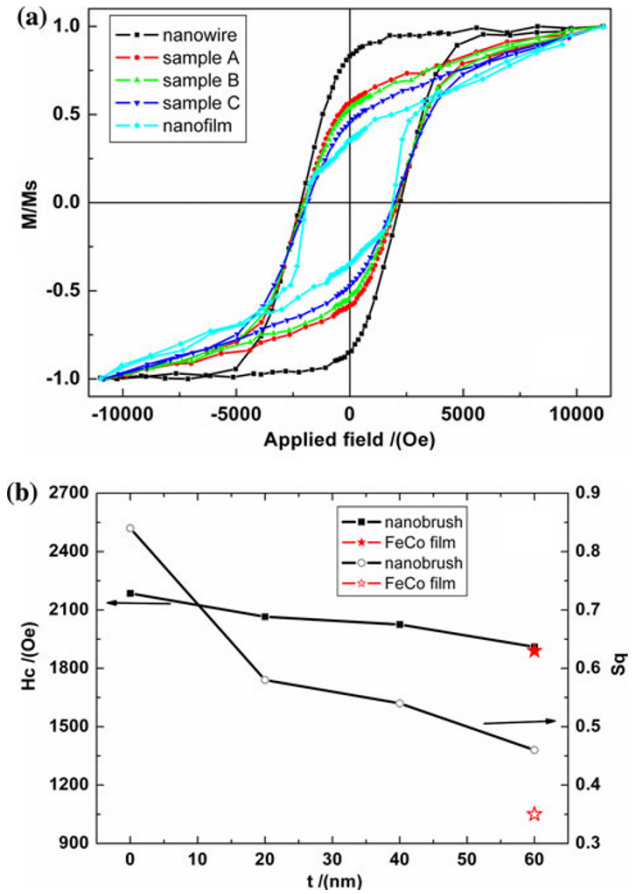

Fig. 3 **a** Normalized hysteresis loops of Co nanowire array, nanobrushes, and nanofilm, **b** Coercivity and Sq of nanobrush as a function of the thickness of nanofilm with the applied field perpendicular to the surface of membrane

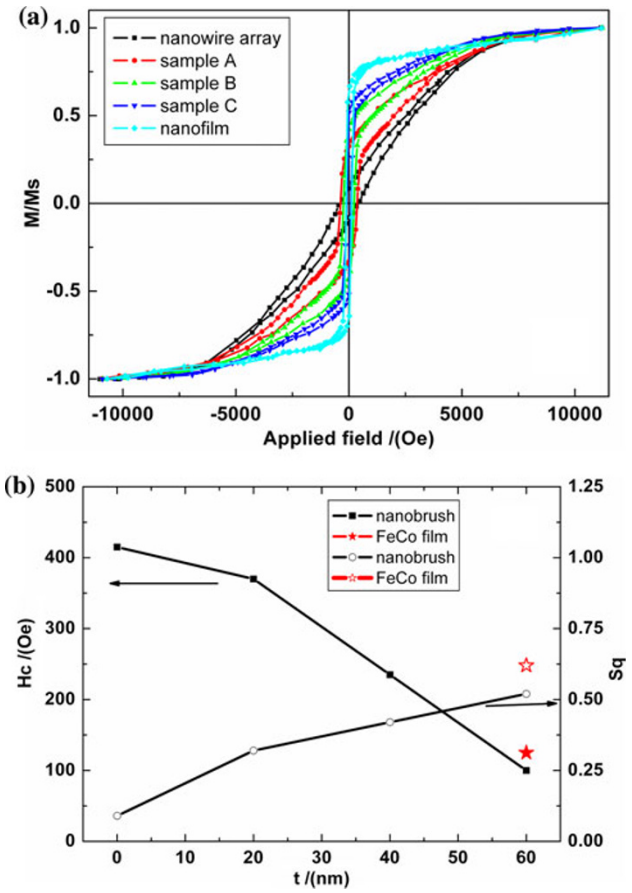

Fig. 4 **a** Normalized hysteresis loops of Co nanowire array, nanobrushes, and nanofilm **b** Coercivity and Sq of nanobrush as a function of the thickness of nanofilm with the applied field parallel to the surface of membrane

magnetic nanobrush by adjusting the thickness of magnetic film. In order to prove this result, micromagnetic simulation was applied to study the magnetization reversal processes of magnetic nanobrush and Co nanowire arrays.

Figure 5 shows normalized hysteresis loops of nanobrush and Co nanowire arrays with the applied paralleled to the long axis of wire, and their magnetic moment distributions at the applied field of 2700 Oe were also shown in the Fig. 5 via micromagnetic simulation. The result also indicates that the magnetic property of nanobrush is determined by the competition of magnetic anisotropy between magnetic film and wires. Firstly, the magnetic moment of nanobrush combining film with wires is out-of-plane and does not parallel the long axis of wires. These magnetic moments are the natural nucleation in the magnetization reversal process of nanobrush, which makes the reversal process easier. To make the magnetization reversal processes of magnetic nanobrush clear, we also simulate the hysteresis loop of Co nanowire arrays. It is found that the coercivity and Sq of nanobrush are lower than those of Co nanowire arrays, which agree well with the experimental results. As well known, the magnetic moment of nanofilm lies in the plane for its shape anisotropy, the magnetic moments of nanowire are along the long axis of wire for the same reason. OOMMF simulation result shows that the direction of the magnetic moment in the film relies on the magnetic moment at the end of wire that is close to the film. It will incline to the $+Z$ direction if the magnetic moment of the end part wire is parallel to the $+Z$ direction, while incline to the $-Z$ direction parallel to the $-Z$ direction. Thus, the magnetic moment will be like a consecutive U-shaped semicircle shown in the Fig. 5 for the two wires with anti-parallel magnetic moment direction and film links them, which lead to the interaction of neighbored wires increases. Furthermore, we chose point A and point B corresponding to the magnetic moments of nanowire array and nanobrush at the applied field of -2700 Oe in Fig. 5. For the nanowire arrays, all the magnetic moments of sixteen nanowires align along the $+Z$ direction at point A, whereas the magnetic moments of eleven nanowire align along the $+Z$ direction and the other five along the $-Z$ direction in nanobrush as shown at point B.

Table 1 The effective anisotropy field of nanowire, nanofilm, and nanobrush with different thickness of $Fe_{70}Co_{30}$ layer

Samples	Nanowire	A	B	C	Nanofilm
Effective anisotropy field (easy axis type)	4270 Oe	740 Oe			
Effective anisotropy field (easy plane type)			900 Oe	2560 Oe	3930 Oe

Sample A, Sample B, and Sample C means nanobrush with 20, 40, and 60 nm thickness of $Fe_{70}Co_{30}$ layer, respectively

The result means that the magnetic moments of five wires reversed in nanobrush and no one reversed in nanowire arrays at the applied field of −2700 Oe. Figure 5 also demonstrates that the adverse fields of nanobrush and nanowire arrays are 1900 Oe and 2700 Oe, respectively. Thus, the magnetic moment of nanowire arrays in nanobrush can be reversed easily compared with the general nanowire arrays. These also agree with the magnetic measurement results that magnetic layer sputtered on the nanowire arrays film will be propitious to the magnetization reversal of nanowire arrays.

Conclusions

Nanobrushes have been synthesized via the bottom-up assemble process. The magnetic hysteresis loops of nanobrushes show their magnetic properties depend on the thickness of $Fe_{70}Co_{30}$ layer. The magnetic anisotropy of nanobrush is similar to nanowire arrays with thinner $Fe_{70}Co_{30}$ layer, while similar to nanofilm with thicker $Fe_{70}Co_{30}$ layer. Micromagnetic simulation also proves that the presence of magnetic nanofilm will assist in the magnetization reversal of nanowire arrays. However, $Fe_{70}Co_{30}$ nanofilms have not a preferred growth orientation in plane; thus, the magnetic moment of $Fe_{70}Co_{30}$ nanofilms is isotropic in the surface of membrane. We believe that the controllability of anisotropy of nanobrush will enhance if the magnetic moment of magnetic layer is uniaxial anisotropy in plane; and magnetic nanobrush may be used as function device with tunable magnetic anisotropy.

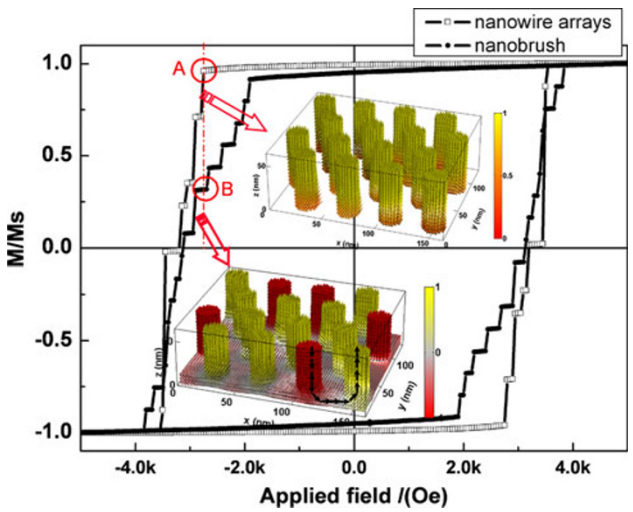

Fig. 5 Normalized hysteresis loops of FCC Co nanowire arrays and nanobrush with the applied field parallel to the long axis of wire via micromagnetic simulation. Magnetic moments distribute for **a** nanowire arrays and **b** nanobrush with the applied field of 2700 Oe

Acknowledgments This work is supported by Program for New Century Excellent Talents (NCET) in University, the National Science Fund for Distinguished Young Scholars (Grant No. 50925103), and the Open Project Program of Low Dimensional Materials & Application Technology (Xiangtan University), Ministry of Education.

References

1. S. Sun, C.B. Murray, D. Weller, L. Folks, A. Moser, Science **287**, 1989 (2000)
2. C.T. Black, C.B. Murray, R.L. Sandstrom, S. Sun, Science **290**, 1131 (2000)
3. T. Thurn-Albrecht, J. Schotter, G.A. Kastle, N. Emley, T. Shibauchi, L. Krusin-Elbaum, K. Guarini, C.T. Black, M.T. Tuominen, T.P. Russell, Science **290**, 2126 (2000)
4. J.B. Yi, L. Shen, H. Pan, L.H. Van, S. Thongmee, J.F. Hu, Y.W. Ma, J. Ding, Y.P. Feng, J. Appl. Phys. **105**, 07C513 (2009)
5. V.F. Puntes, K.M. Krishnan, P. Alivisatos, Appl. Phys. Lett. **78**, 2187 (2001)
6. Y. Ren, Q.F. Liu, S.L. Li, J.B. Wang, X.H. Han, J. Magn. Magn. Mater. **321**, 226 (2009)
7. S.I. Woods, J.R. Kirtley, S. Sun, R.H. Koch, Phys. Rev. Lett. **87**, 137205 (2001)
8. W.L. Zhang, R.J. Tang, H.C. Jiang, W.X. Zhang, B. Peng, H.W. Zhang, IEEE Trans. Magn. **41**, 4390 (2005)
9. J.H. Gao, Q.F. Zhan, W. He, D.L. Sun, Z.H. Cheng, J. Magn. Magn. Mater. **305**, 365 (2006)
10. Y. Ren, J.B. Wang, Q.F. Liu, B. Zhang, X.H. Han, D.S. Xue, J. Phys. D Appl. Phys. **42**, 105002 (2009)
11. Y.H. Huang, H. Okumura, G.C. Hadjipanayis, D. Weller, J. Appl. Phys. **91**, 6869 (2002)
12. P.D. McGary, L. Tan, J. Zou, B.J.H. Stadler, P.R. Downey, A.B. Flatau, J. Appl. Phys. **99**, 08B310 (2006)
13. J. Yuan, W. Pei, T. Hasagawa, T. Washiya, H. Saito, S. Ishio, H. Oshima, K.-i. Itoh, J. Magn. Magn. Mater. **320**, 736 (2008)
14. F.S. Li, T. Wang, L.Y. Ren, J.R. Sun, J. Phys.: Condens. Matter **16**, 8053 (2004)
15. M. Darques, A. Encinas, L. Vila, L. Piraux, J. Phys. D Appl. Phys. **37**, 1411 (2004)

16. B. Das, K. Mandal, P. Sen, S.K. Bandopadhyay, J. Appl. Phys. **103**, 013908 (2008)
17. J.B. Wang, X.Z. Zhou, Q.F. Liu, D.S. Xue, F.S. Li, B. Li, H.P. Kunkel, G. Williams, Nanotechnology **15**, 485 (2004)
18. R. Ferre, K. Ounadjela, J.M. George, L. Piraux, S. Dubois, Phys. Rev. B **56**, 14066 (1997)
19. V.A. Antohe, A. Radu, M. Matefi-Tempfli, A. Attout, S. Yunus, P. Bertrand, C.A. Dutu, A. Vlad, S. Melinte, S. Matefi-Tempfli, L. Piraux, Appl. Phys. Lett. **94**, 073118 (2009)
20. Z. Fan, J.C. Ho, Z.A. Jacobson, H. Razavi, A. Javey, Proc. Natl. Acad. Sci. **105**, 11066 (2008)
21. X. Wu, H. Li, L. Chen, X. Huang, Solid State Ionics **149**, 185 (2002)
22. Y. Huang, X. Duan, Q. Wei, C.M. Lieber, Science **291**, 630 (2001)
23. H. Masuda, K. Fukuda, Science **268**, 1466 (1995)
24. X.H. Han, Q.F. Liu, J.B. Wang, S.L. Li, Y. Ren, R.L. Liu, F.S. Li, J. Phys. D Appl. Phys. **42**, 095005 (2009)